

Hexabenzocoronene Model Compounds for Asphaltene Fractions: Synthesis & Characterization

Felaniaina Rakotonradany,^{†,‡} Hicham Fenniri,^{*,‡} Parviz Rahimi,[§] Keith L. Gawrys,^{||}
Peter K. Kilpatrick,^{||} and Murray R. Gray^{*,†}

*Department of Chemical and Materials Engineering, University of Alberta, Edmonton, Alberta, Canada,
Department of Chemistry and National Institute for Nanotechnology, University of Alberta, Edmonton,
Alberta, Canada, National Centre for Upgrading Technology, Devon, Alberta, Canada, and Department of
Chemical and Biomolecular Engineering, North Carolina State University, Raleigh, North Carolina*

Received March 28, 2006. Revised Manuscript Received July 30, 2006

Asphaltenes are the fraction of bitumen with the highest molecular weight, containing polyaromatic hydrocarbons rich in heteroatoms and polar groups that result in strong self-association under extraction and upgrading conditions. The synthesis of alkylated hexabenzocoronenes is here reported to provide new insight into the behavior of bitumen residue fractions. The self-association behavior of these polyaromatic model compounds is investigated over a range of temperatures using vapor pressure osmometry (VPO), nuclear magnetic resonance (NMR), optical and electron microscopy, X-ray and small-angle neutron scattering, and calorimetry (DSC/TGA). In addition to these experimental studies, computational studies are used to determine the contribution of alkyl–alkyl and π – π stacking interactions to this association behavior. Experimental and computational results are compared to asphaltene properties under extraction and upgrading conditions, as well as to the archipelago and pericondensed models proposed for asphaltenes.

Introduction

Asphaltenes, which are the highest molecular weight fraction of bitumen and heavy oils, are an extremely complex mixture of polycyclic aromatic hydrocarbons rich in heteroatoms and polar groups. The interaction of these components gives rise to the strong self-association of asphaltene molecules under bitumen extraction and upgrading conditions. The resulting precipitation, flocculation, and coke formation can cause partial or complete blockage of production facilities and poison refinery catalysts, dramatically affecting crude oil recovery and product yields.

The tendency of asphaltene to self-associate is problematic because it impedes the separation of asphaltenes into distinct chemical species, and consequently, the characterization of the chemical and physical behavior of these molecules in bitumen and heavy oil. Although two types of molecular models have been proposed, the chemical identity of asphaltene remains unknown. In the pericondensed model,¹ large polyaromatic sheets are surrounded by alkyl and alkylthiol chains, while in the archipelago model² aromatic and naphthenic moieties are linked through alkyl and thioether bridges. Colloidal and

polymeric models have also been proposed to explain the associative behavior of asphaltenes using rheology, vapor-pressure osmometry (VPO),³ and calorimetry. However, the lack of reliable reference compounds for asphaltene molecules hinders a precise identification of the aggregation mechanisms.

Another method to understand the molecular structure and self-association of asphaltenes is to design and synthesize pure compounds containing the functional groups that have been identified in previously reported analytical studies.^{1,2} The ability of these model compounds to self-associate can then be investigated under extraction and upgrading conditions and related to asphaltene behavior under similar conditions.⁴

A series of polynuclear aromatic hydrocarbons using four-ring pyrenyl derivatives have recently been synthesized and investigated in our research group.⁴ In these model structures, the aromatic rings were linked or bridged through alkyl and oxygen-containing polar chains to allow hydrogen-bonding, alkyl–alkyl, and π – π stacking interactions between the molecules. Investigation of these model compounds in solution showed little self-association. Some association was observed in the oxygen-containing pyrene derivatives, indicating the importance of polar groups for self-aggregation. Nonetheless, these studies clearly suggested that larger alkyl polynuclear aromatic hydrocarbons need to be designed and synthesized to enhance self-association significantly.

(2) For examples of archipelago models for asphaltenes, see: (a) Murgich, J.; Abanero, J. A.; Strausz, O. P. *Energy Fuels* **1999**, *13*, 278–286. (b) Sheremata, J. M.; Gray, M. R.; Dettman, H. D.; McCaffrey, W. C. *Energy Fuels* **2004**, *18*, 1377–1384.

(3) Agrawala, M.; Yarranton, H. W. *Ind. Eng. Chem. Res.* **2001**, *40*, 4664–4672.

(4) Akbarzadeh, K.; Bressler, D. C.; Wang, J.; Gawrys, K. L.; Gray, M. R.; Kilpatrick, P. K.; Yarranton, H. W. *Energy Fuels* **2005**, *19*, 1268–1271.

* To whom correspondence should be addressed. E-mail: hicham.fenniri@nrc-cnrc.gc.ca (H.F.); murray.gray@ualberta.ca (M.R.G.). Phone: 780-492-8988 (H.F.); 780-492-7965 (M.R.G.). Fax: 780-492-8632 (H.F.); 780-492-2881 (M.R.G.).

[†] Department of Chemical and Materials Engineering, University of Alberta.

[‡] Department of Chemistry and National Institute for Nanotechnology, University of Alberta.

[§] National Centre for Upgrading Technology.

^{||} Department of Chemical and Biomolecular Engineering, North Carolina State University.

(1) For examples of pericondensed models for asphaltenes, see: (a) Groenzin, H.; Mullins, O. C. *Energy Fuels* **2000**, *14*, 677–684. (b) Zhao, S.; Kotlyar, L. S.; Woods, J. R.; Sparks, B. D.; Hardacre, K.; Chung, K. H. *Fuel* **2001**, *80*, 1155–1163.

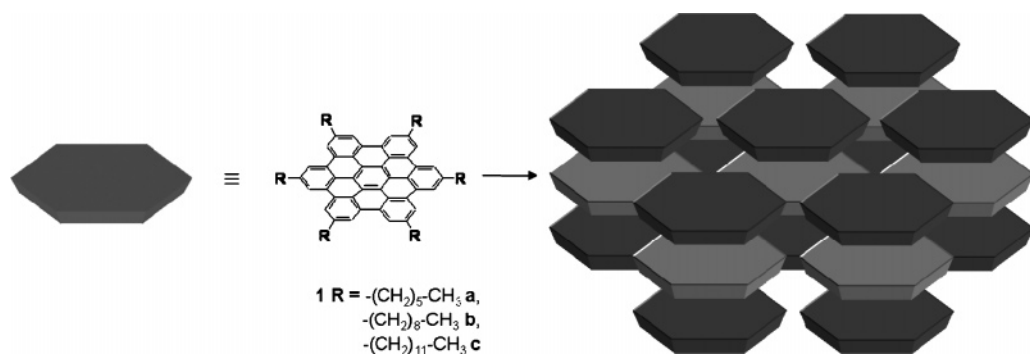


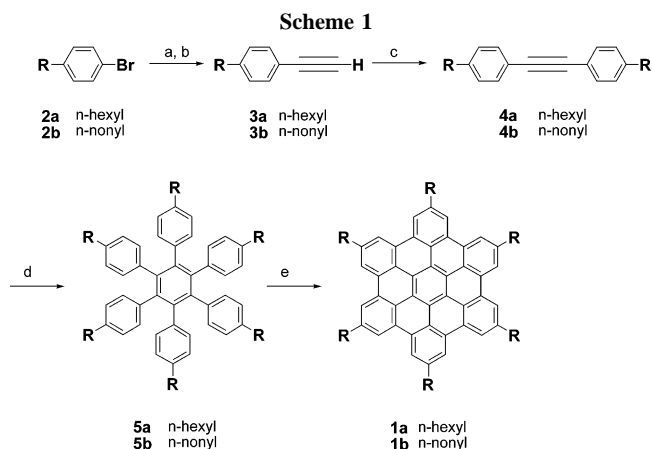
Figure 1. Self-assembly of hexasubstituted hexabenzocoronene **1**.

Alkyl hexabenzocoronene (HBC) derivatives,⁵ like C₁₂-HBC **1c** (Figure 1), have recently been shown to strongly self-associate in solution, where the interplay of alkyl-alkyl and π - π stacking interactions controls the orientation of these discotic molecules. The resulting liquid crystalline phases were found to be stable above the thermal stability limit of the molecules (>400 °C) (Figure 1). Here we report the synthesis of C₆- and C₉-hexasubstituted hexabenzocoronenes **1a** and **1b** as model compounds for asphaltene fractions (Figure 1). The associative properties of the thirteen-ring pericondensed molecule **1a** were determined using vapor-pressure osmometry (VPO), ¹H NMR, differential scanning calorimetry, thermogravimetric analysis, hot-stage polarized microscopy, scanning electron microscopy, and X-ray and small-angle neutron scattering. The results were related to the behavior of asphaltenes under bitumen extraction and upgrading conditions, allowing a test of the validity of the pericondensed model proposed for the asphaltenic fraction.¹ Molecular modeling studies were also performed to gain additional insight into the self-association properties of **1a**.

Results and Discussion

Synthesis of C₆- and C₉-Hexabenzocoronenes. C₆- and C₉-hexasubstituted hexabenzocoronenes **1a** (C₆-HBC) and **1b** (C₉-HBC) were synthesized following Scheme 1.⁶ The para-substituted bromobenzene derivatives, **2**, were first reacted with trimethylsilylacetylene under Sonogashira coupling conditions and deprotected to give the alkynyl derivatives **3**. Compounds **3** were subjected to a second Sonogashira coupling reaction with **2** to give the diphenylacetylenes **4**. Trimerization using Co₂(CO)₈ in dioxane followed by aromatization yielded the desired hexabenzocoronene derivatives, which were characterized by NMR and mass spectrometry (see Supporting Information for details).

Aggregation Properties of C₆-Hexabenzocoronene (1a). *Vapor-Pressure Osmometry Studies.* Vapor-pressure osmometry (VPO) measurements of C₆-HBC **1a** were carried out in toluene at 75 °C and in *o*-dichlorobenzene at 100 °C, using benzil ($M_n = 210$), 1,10-dipyrenyldecane ($M_n = 542$), and polystyrene ($M_n = 820$) as molecular weight standards. (Figure 2) The apparent molecular weights of C₆-HBC **1a** increased linearly with concentration in toluene, indicating that C₆-HBC **1a** forms dimers, trimers, and other oligomers in this solvent. The y intercepts were obtained at $M_n = 1875$ using benzil and at M_n



(a) Trimethylsilylacetylene, PdCl₂(PPh₃)₂, CuI, PPh₃, piperidine, 80 °C; (b) KF, DMF; (c) **2**, Pd (PPh₃)₄, CuI, Piperidine, 80 °C; (d) Co₂(CO)₈, 1,4-dioxane, reflux; (e) FeCl₃, CH₃NO₂, CH₂Cl₂, room temperature.

= 1895 using polystyrene, consistent with the formation of hexabenzocoronene dimers ($M_n = 2052$) at infinite dilution in toluene.

The apparent molecular weights showed little concentration dependence in *o*-dichlorobenzene. (Figure 2) However, y intercepts corresponding to $M_n = 1675$ using benzil and $M_n = 1898$ using 1,10-dipyrenyldecane were obtained at infinite dilution by linear regression, suggesting the coexistence of hexabenzocoronene **1a** monomers and dimers in this solvent at 100 °C. This observation suggests that if asphaltenes contain structures similar to hexabenzocoronene, then they may not completely dissociate in *o*-dichlorobenzene. These data support the contention of Wiehe⁷ that use of a strong solvent at elevated temperature will minimize association, but they also suggest that VPO can overestimate the molecular weight of asphaltene molecules even when multiple measurements show no significant change with concentration.

Both C₆-HBC **1a** and Athabasca asphaltenes in toluene showed two concentration-dependent domains of self-association (Figure 2). The apparent molecular weights for the asphaltenes increase in a nonlinear fashion for concentrations below 3 g/L, then rise linearly as a function of concentration.⁸ Similarly, the apparent molecular weights for C₆-HBC **1a** increased from the true value of 1026 to 2100 at 3 g/L, then more slowly as concentration was increased. When a polymeric model for the association is used, the apparent molecular weights obtained

(5) (a) Watson, M. D.; Fechtenkötter, A.; Müllen, K. *Chem. Rev.* **2001**, *101*, 1267–1300. (b) Ito, S.; Wehmeier, M.; Brand, J. D.; Kübel, C.; Epsch, R.; Rabe, J. P.; Müllen, K. *Chem.-Eur. J.* **2000**, *6*, 4327–4342. (c) Tchebotareva, N.; Yin, Y.; Watson, M. D.; Samori, P.; Rabe, J. P.; Müllen, K. *J. Am. Chem. Soc.* **2003**, *125*, 9734–9739.

(6) Brown, S. P.; Schnell, I.; Brand, J. D.; Müllen, K.; Spiess, H. W. *J. Am. Chem. Soc.* **1999**, *121*, 6712–6718.

(7) Wiehe, I. A. *Ind. Eng. Chem. Res.* **1992**, *31*, 530–536.

(8) The error in the VPO determination is substantial for concentrations below 3 g/L, as illustrated by replicates in the C5 asphaltene data at 1 g/L ($M_n = 2881$ and 3687) and 2 g/L ($M_n = 3633$ and 4576). Data points for C₆-HBC for concentrations below 3 g/L are not reported because of this significant experimental error associated with concentration range.

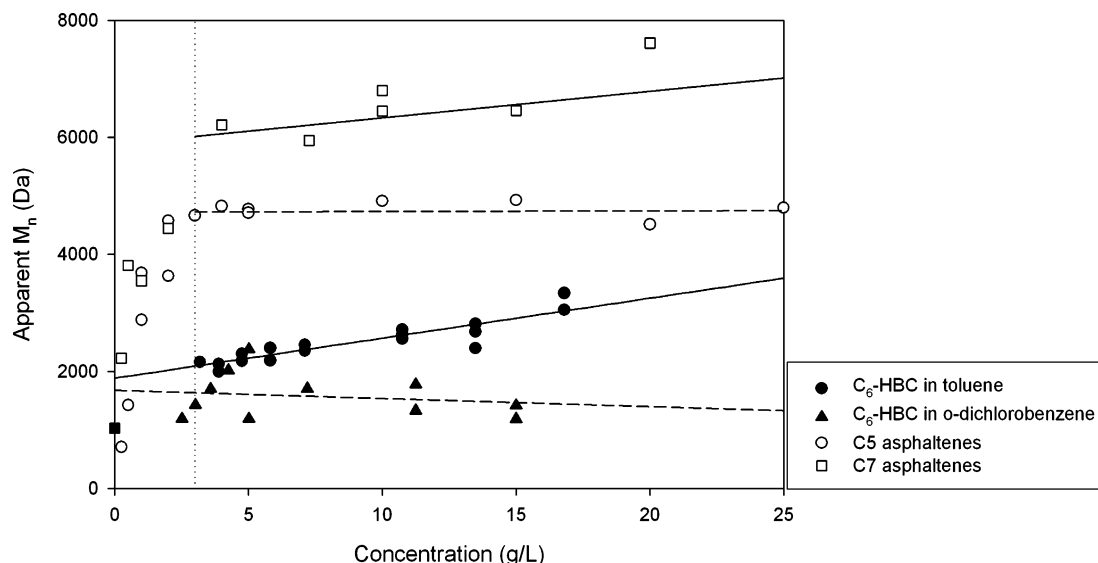


Figure 2. Vapor pressure osmometry of C_6 -HBC in toluene ($T = 70\text{--}75\text{ }^\circ\text{C}$) (\bullet) and in *o*-dichlorobenzene ($T = 100\text{ }^\circ\text{C}$) (\blacktriangle), along with C5 (\circ) and C7 (\square) Athabasca asphaltenes in toluene ($T = 70\text{--}75\text{ }^\circ\text{C}$).³ (\blacksquare) Theoretical molecular weight for a C_6 -HBC monomer.

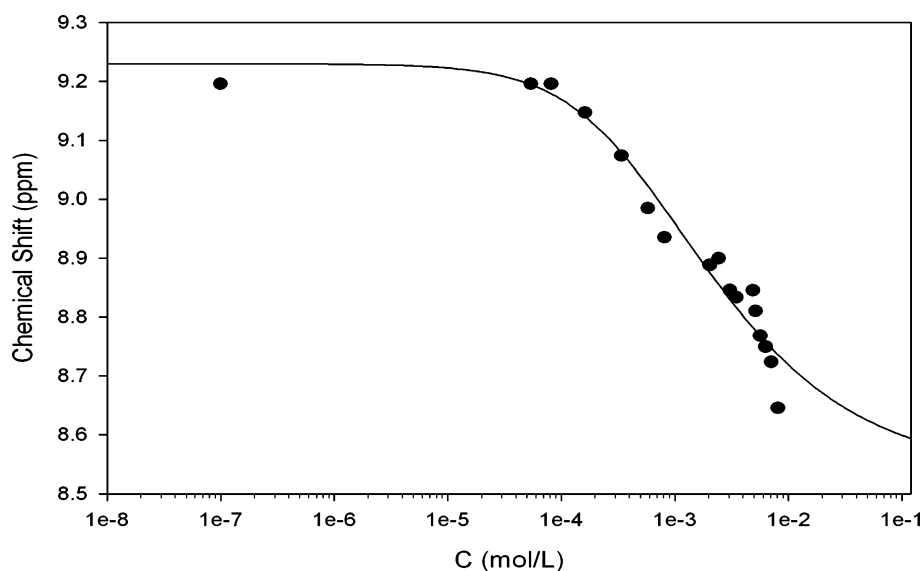


Figure 3. Concentration-dependent ^1H NMR chemical shifts of the aromatic C_6 -HBC peak in toluene- d_8 ($T = 25\text{ }^\circ\text{C}$), fitted with an indefinite self-association model.¹⁰

for C5 and C7 Athabasca asphaltenes start at ~ 1500 and 1600 , respectively, at infinite dilution, then follow a 4-fold increase to ~ 4700 and 6000 at 3 g/L . Although similar apparent molecular weights are calculated for C_6 -HBC at infinite dilution in toluene, the M_n values for C_6 -HBC reach ~ 2000 only at 3 g/L , suggesting a greater tendency for asphaltenes to self-associate in comparison with C_6 -HBC at low concentrations. However, in the $3\text{--}20\text{ g/L}$ range this trend was inverted, indicating that C_6 -HBC tends to associate more strongly than Athabasca asphaltenes at higher concentrations.

NMR Studies. The self-association behavior of C_6 -HBC **1a** was investigated by measuring its ^1H NMR spectra at concentrations ranging from 10^{-2} mol/L and 10^{-7} mol/L in toluene- d_8 at $25\text{ }^\circ\text{C}$. Examination of the aromatic region showed a significant downfield shift of ~ 0.6 ppm for these peaks upon dilution, accompanied by a peak sharpening (Figure 3). This concentration-dependent shift of the aromatic protons is characteristic of π - π stacking interactions in solution and agrees with previous studies on HBC molecules.⁹ A least-squares nonlinear fit was performed using an indefinite self-association

model taking nearest-neighbor interactions into account.¹⁰ The resulting sigmoid reached a plateau around 10^{-5} mol/L (0.01 g/L), suggesting the presence of monomers, thus full dissociation, below this concentration.¹¹ Analysis of the concentration range from 10^{-2} to 10^{-5} mol/L ($10\text{--}0.01\text{ g/L}$) indicated that the preponderance of C_6 -HBC formed dimers in solution,¹⁰ in agreement with the VPO results. Asphaltenes have been reported to aggregate at concentrations as low as 0.10 g/L ,¹² as determined by ultrasonic spectrometry in toluene, and to form dimers at 0.05 g/L .¹³ C_6 -HBC **1a** began aggregating at the more dilute condition of 0.01 g/L . This difference in the aggregation

(9) (a) Shetty, A. S.; Zhang, J.; Moore, J. S. *J. Am. Chem. Soc.* **1996**, *118*, 1019–1027. (b) Kastler, M.; Pisula, W.; Wasserfallen, D.; Pakula, T.; Müllen, K. *J. Am. Chem. Soc.* **2005**, *127*, 4286–4296.

(10) Martin, R. B. *Chem. Rev.* **1996**, *96*, 3043–3064.

(11) The apparent discrepancy between this ^1H NMR data and the apparent value of M_n for **1a** measured by VPO at infinite dilution is linked to the poor detection limit of VPO below 3 g/L requiring the use of linear regression (see ref 8).

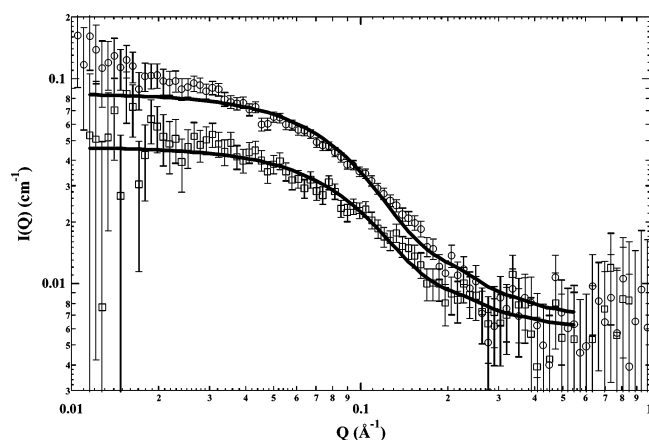
(12) Andreatta, G.; Goncalves, C. C.; Buffin, G.; Bostrom, N.; Quintella, C. M.; Arteaga-Larios, F.; Perez, E.; Mullins, O. C. *Energy Fuels* **2005**, *19*, 1282–1289.

Table 1. SANS Model Fitting Parameters for HBC in toluene- d_8 Using the Guinier Analysis and the Monodisperse Oblate Cylinder Model (in parentheses)

concentration (g/L)	ϕ_{solute}	I_0 (cm^{-1})	R (\AA)	L (\AA)	R_G (\AA)	M_w (Da)
6.3 ± 0.7	0.0066 ± 0.0007	0.148 ± 0.002 (0.078 ± 0.002)	(24.9 ± 0.5)	(5 ± 1)	19.0 ± 0.7 (18 ± 4)	6000 ± 1000 (3100 ± 600)
3.2 ± 0.4	0.0032 ± 0.0004	0.099 ± 0.002 (0.040 ± 0.002)	(23.3 ± 0.9)	(5 ± 1)	14.1 ± 0.6 (17 ± 4)	8000 ± 1000 (3200 ± 700)

onset concentrations might be caused by the complexity of the asphaltene mixtures, but it also may be the result of the possible steric interference of bridged archipelago structures.

Small-Angle Neutron Scattering. Scattering intensity versus scattering angle ($I(Q)$ vs Q) curves for 6.3 g/L and 3.2 g/L solutions of C₆-HBC **1a** in toluene- d_8 at 20 °C are shown in Figure 4. The radii of gyration of the C₆-HBC **1a** aggregates

**Figure 4.** Small-angle neutron scattering intensity curves for 6.3 g/L (○) and 3.2 g/L (□) solutions of C₆-HBC in toluene- d_8 . Solid lines represent fits to monodisperse oblate cylinder.

were determined to be 19.0 ± 0.7 and 14.1 ± 0.6 Å by Guinier analysis.¹⁴ The value of $I(Q = 0)$ or I_0 is related to the weight-average molecular weight of the aggregates by the equation

$$M_w = \frac{I_0 N_A d_m}{\phi(\Delta\rho)^2}$$

where N_A is Avogadro's number, d_m is the scatterer mass density (~ 0.95 g/cm³), ϕ is the scatterer volume fraction, and $\Delta\rho$ is the scattering contrast term estimated using the chemical compositions of the solute and the solvent. Guinier analysis provides significantly higher values for I_0 , giving rise to molecular weights of $M_w = 6000 \pm 1000$ Da and $M_w = 8000 \pm 1000$ for the 6.3 g/L and 3.2 g/L C₆-HBC samples, respectively. These M_w values obtained by Guinier analysis suggest the formation of hexameric to octameric aggregates.

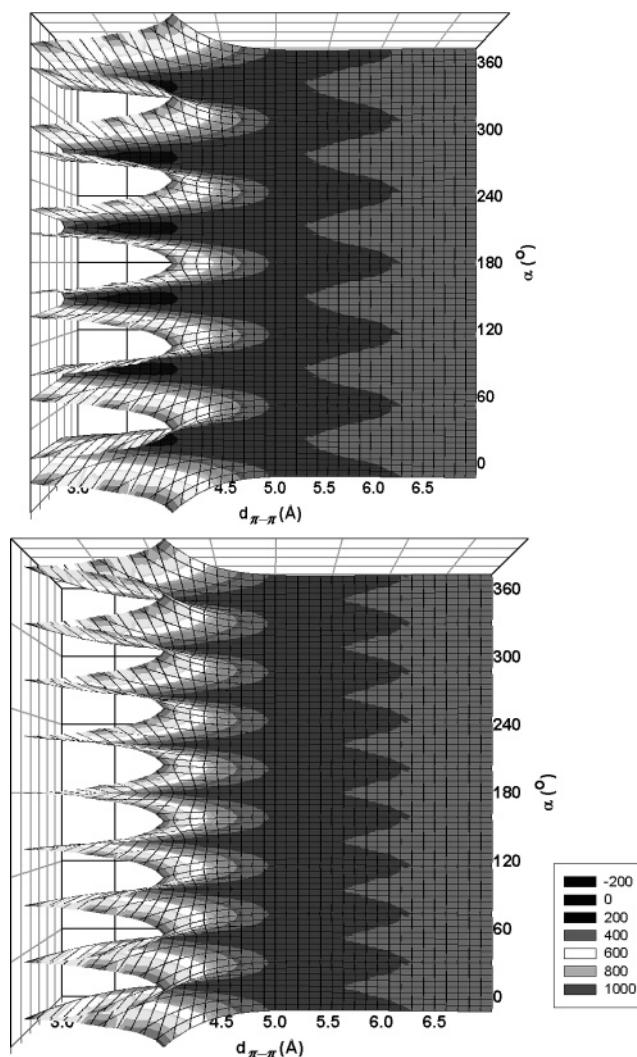
Recent small-angle neutron scattering studies of asphaltenes have suggested polydisperse oblate cylinder models to best fit the shape of asphaltenic aggregates.¹⁵ With a monodisperse oblate cylinder form factor,¹⁶ the radius of gyration of the C₆-HBC aggregates was calculated as 18 ± 4 Å, in agreement with the Guinier analysis. The aggregate molecular weight obtained from the parameters in Table 1 is $M_w \approx 3200 \pm 600$ which

(13) Goncalves, S.; Castillo, J.; Fernandez, A.; Hung, J. *Fuel* **2004**, *83*, 1823–1828.

(14) Guinier, A. *Small Angle Scattering of X-rays*; Wiley: New York, 1955.

(15) Gawrys, K. L.; Kilpatrick, P. K. *J. Colloid Interface Sci.* **2005**, *288*, 325–334.

(16) (a) Pedersen, J. S. *Adv. Colloid Interface Sci.* **1997**, *70*, 171–210. (b) Pedersen, J. S. *J. Appl. Crystallogr.* **2000**, *33*, 637–640.

**Figure 5.** Total energy profiles as a function of the relative rotation of the stacked rings about the z axis, α and the interplanar distances along the z axis, $d_{\pi-\pi}$ in the absence of horizontal offset ($\sigma_{\pi-\pi} = 0$). Nonhelical (a) and helical (b) arrangements of C₆-HBC **1a** molecules.

corresponds to the formation of trimers, in close agreement with the apparent molecular weights of C₆-HBC observed by VPO at these concentrations.¹⁷

Molecular Modeling. The experimental characterization of C₆-HBC by osmometry, NMR, calorimetry, SANS, and STEM (vide infra) revealed the presence of molecular aggregates, suggesting favorable alkyl–alkyl and π -stacking interactions between these hexabenzocorone derivatives. The face-packing arrangement of these hexabenzocorones by stacking along the axis normal to the polycyclic aromatic hydrocarbons would give rise to columnar or lamellar structures in the bulk (Figure 1). The close-packing arrangement of the hexabenzocoronene

(17) The differences in the SANS molecular weights stem directly from differences in the I_0 values determined using the two models, assuming all other parameters are constant.

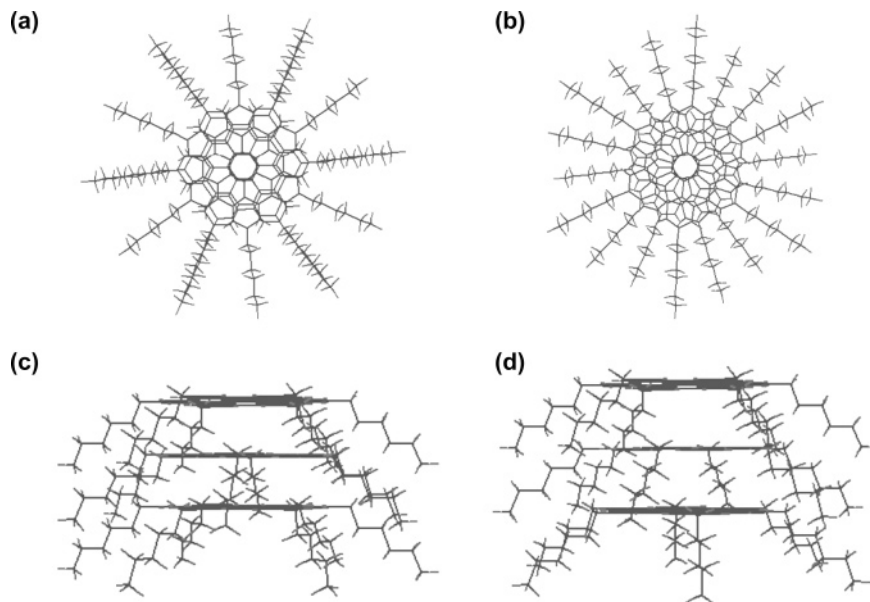


Figure 6. Optimal face-to-face packing of bowl-like hexabenzocoronene: nonhelical arrangements (a) top view, (c) side view; helical arrangements (b) top view, (d) side view.

derivatives was optimized using a very simple molecular model. The structure of a single C_6 -HBC molecule was first optimized using PM3. The interactions of two and three C_6 -HBC molecules were then analyzed as stacks in a face-to-face configuration along the z axis.¹⁸ Simple single-point calculations were carried out using MM⁺ for these one-dimensional hexabenzocoronene arrays, as a function of the relative rotation of the stacked rings about the z axis, α , and the interplanar distances along the z axis, $d_{\pi-\pi}$, and the horizontal offset, $o_{\pi-\pi}$, for nonhelical and helical arrangements of C_6 -HBC molecules to generate total energy profiles.

The calculated energy plots for the stacked molecules (Figure 5) show an overall energy decrease with increasing interplanar distances for all the polyaromatic ring conformations, which levels off to a minimum beyond 4.5–5.0 Å, consistent with strong electrostatic repulsions between the negatively charged HBC π -systems at short distances. The energy scan for α was performed by varying the position of the middle hexabenzocoronene between 0 and 30° while keeping the top/bottom hexabenzocoronenes immobile for nonhelical structures,¹⁹ as a full 360° rotation around the z axis can be produced through symmetry operations. The resulting energy plots show a $\pi/3$ periodicity over the angular range, consistent with the 6-fold symmetry of the hexabenzocoronene backbone. A sequence of local energy minima were obtained which were more pronounced in close-packed systems ($d_{\pi-\pi} = 3.0$ – 4.5 Å) than at greater interplanar distances. These local minima occur at 30, 90, 150, 210, 270, and 330° in nonhelical arrangements which correspond to configurations in which the alkyl chains are the furthest from one another, suggesting unfavorable steric effects between the peripheral substituents. These steric effects are more pronounced in helical systems, where shallow energy minima are observed at interplanar distances greater than 4.0 Å. The effect of translation within the xy plane, $o_{\pi-\pi}$, on the total energy of three stacked molecules was also calculated over a small

distance interval.²⁰ The total energy plots against the horizontal translation $o_{\pi-\pi}$ decreased with increasing translational distances at greater interplanar distances, emphasizing the steric effects of the alkyl chains on close-packing.

Overall, the calculations of the total energy show that the interplanar distance, $d_{\pi-\pi}$, and the aromatic ring rotation, α , contribute to the face-to-face packing of hexabenzocoronene to a greater extent than the horizontal offset, $o_{\pi-\pi}$. Close-packing should therefore be favorably achieved for interplanar distances of 3.5 Å and relative rotations of 30° about the z axis for nonhelical arrangements (Figure 6a and c). In helical arrangements, interplanar distances of 4.3 Å and relative rotations of 20° about the z axis should give close-packed hexabenzocoronenes (Figure 6b and d). The calculations for the dimeric stacks of alkyl hexabenzocoronene gave similar energy profiles and therefore similar minimum energy geometries. However, the total energies observed for the dimers were 40 kcal/mol lower than for the trimers, suggesting their greater stability compared with the trimers. This result is in good agreement with the apparent molecular weight of C_6 -HBC determined by vapor pressure osmometry at infinite dilution and the association data from ¹H NMR spectrometry.

Hot-Stage Microscopy. The thermal behavior of C_6 -HBC **1a** was monitored by direct observation of crystalline samples by hot-stage optical microscopy. No clear melting temperature was detected upon heating from room temperature to 250 °C, consistent with the DSC results (2–5 °C/min, vide infra). Over this temperature range, the red C_6 -HBC **1a** powder progressively turned into a viscous substance, at the edges of which birefringence could be observed at approximately 200 °C (Figure 7). A similar reduced fluidity has been reported previously and, likewise, was attributed to the N₂ atmosphere used in these studies.^{21,22}

(18) Rakotondradany, F. PhD Thesis, McGill University, 2004. See computational details in the Supporting Information.

(19) For helical arrangements, the energy plots as a function of relative rotation were produced by simultaneously varying the middle macrocycle between 0 and 20° and the lowest macrocycle between 0 and 40°.

(20) A small distance interval equivalent to 1/2 of the hexabenzocoronene core was chosen to evaluate the effect of the horizontal offset on total energies because of the high symmetry of the model compound.

(21) Perrotta, A. J.; McCullough, J. P.; Beuther, H. *Prepr. Pap.-Am. Chem. Soc., Div. Pet. Chem.* **1983**, 633–639.

(22) (a) Rahimi, P.; Gentzis, T.; Dawson, W. H.; Fairbridge, C.; Khulbe, C.; Chung, K.; Nowlan, V.; DelBianco, A. *Energy Fuels* **1998**, *12*, 1020–1030. (b) Rahimi, P.; Gentzis, T. *Energy Fuels* **1999**, *13*, 694–701.

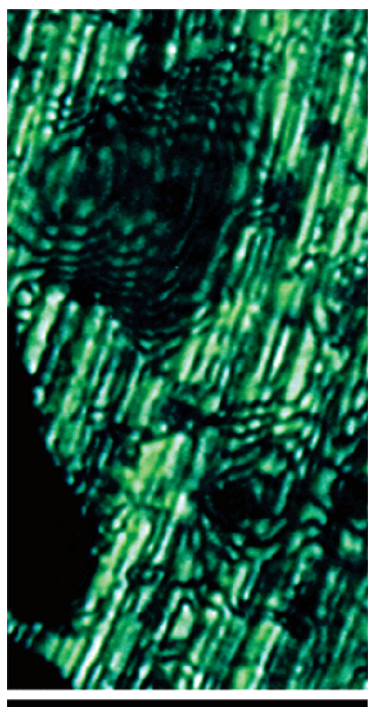
40 μm

Figure 7. Optical micrograph of C_6 -HBC under polarized light (cross-polarizers, green filter) upon heating ($T = 225\text{ }^\circ\text{C}$, N_2 500 psi). The vertical striations are from the metal support.

Although blackening of the melt could be observed starting at $250\text{ }^\circ\text{C}$, the birefringent textures persisted up to approximately $400\text{ }^\circ\text{C}$. Thermal decomposition of the C_6 -HBC sample through significant coke formation was only detected after prolonged heating at $440\text{ }^\circ\text{C}$. The annealed C_6 -HBC samples did not recrystallize upon cooling but remained viscous over several hours ($>24\text{ h}$) after cooling. This thermal behavior is consistent with the high thermal stability observed in similar liquid-crystalline hexabenzocoronenes and in bitumen and heavy-oil fractions.^{8,9}

Unlike C_6 -HBC **1a**, Athabasca bitumen vacuum bottom fractions have been shown by hot-stage microscopy studies to form birefringent species only after prolonged heating at $440\text{ }^\circ\text{C}$ for more than 75 min , with relatively shorter induction periods for asphaltene-rich fractions than for residue fractions rich in resins and aromatics.^{22a} This discrepancy in the thermal behaviors of C_6 -HBC **1a** and vacuum residue can be explained

by their different chemical composition. Vacuum residue fractions can aggregate not only through the alkyl-alkyl and π - π stacking interactions preponderant in C_6 -HBC **1a** but also through strong dipole-dipole interactions and electrostatic forces, thus limiting the ability of the molecules to reorganize in the melt. Alternatively, the original bitumen materials may not contain species capable of forming discotic mesophases, which would be generated only after extensive heating.

Differential Scanning Calorimetry. Both alkyl-HBC model compounds **1a** and **1b** showed similar differential scanning calorimetry profiles upon heating (Figure 8). Although both compounds are solids at room temperature, no endothermic peak was detected within the 30 – $600\text{ }^\circ\text{C}$ temperature range. The transition from mesophase to isotropic liquid was not detected by DSC. These observations suggest that the alkyl-HBC molecules undergo progressive rather than dramatic changes, consistent with the self-associating behavior of alkylated hexabenzocoronenes observed by hot-stage microscopy.

X-ray Diffraction. Two broad features are observed by X-ray diffraction for C_6 -HBC, which could be assigned by analogy with previously reported alkyl hexabenzocoronene diffractograms. Despite the broadness of the observed peaks, characteristic of amorphous materials, the X-ray diffraction pattern of C_6 -HBC closely matched the X-ray diffraction pattern of columnar materials,²³ where the intercolumnar distances are 18.3 \AA ($2\theta = 4.7^\circ$). A broad peak was detected around 4.4 \AA ($2\theta = 20.1^\circ$), which may be attributed to the disordered arrangement of the alkyl chains. The presence of a third shoulder peak allows an estimate of interplanar distances in the 3.5 – 3.6 \AA range ($2\theta = 25.4$ – 25.7°). The broadness of these peaks also suggests the coexistence of different hexabenzocoronene conformations in the measured materials in agreement with the molecular modeling results. X-ray diffractograms of C_6 -HBC powders acquired at temperatures ranging from 24 to $150\text{ }^\circ\text{C}$ are shown in Figure 9. These temperature-dependent measurements showed a pronounced increase in peak intensity upon heating, along with a peak narrowing, around 18 \AA . Application of Scherrer's equation²⁴ to this main peak gave crystal sizes varying from 4.42 to 5.30 nm upon temperature increase. This result is consistent with a heat-induced reorganization of the C_6 -HBC molecules within the stacks leading to increasingly uniform intercolumnar distances. The reordering of C_6 -HBC detected by X-ray diffraction upon heating is in agreement with the hot-stage polarized microscopy results.²⁵

The overlap between the features of C_6 -HBC from the aromatic and alkyl structures around 4.4 \AA ($2\theta = 20.1^\circ$) is in

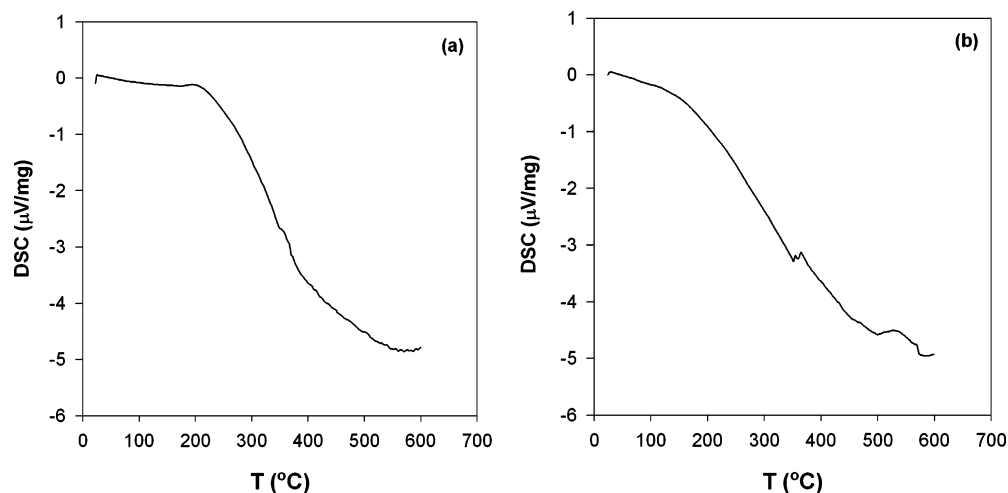


Figure 8. Differential scanning calorimetry of (a) C_6 -HBC **1a** and (b) C_9 -HBC **1b**. Heating rate = $5\text{ }^\circ\text{C}/\text{min}$.

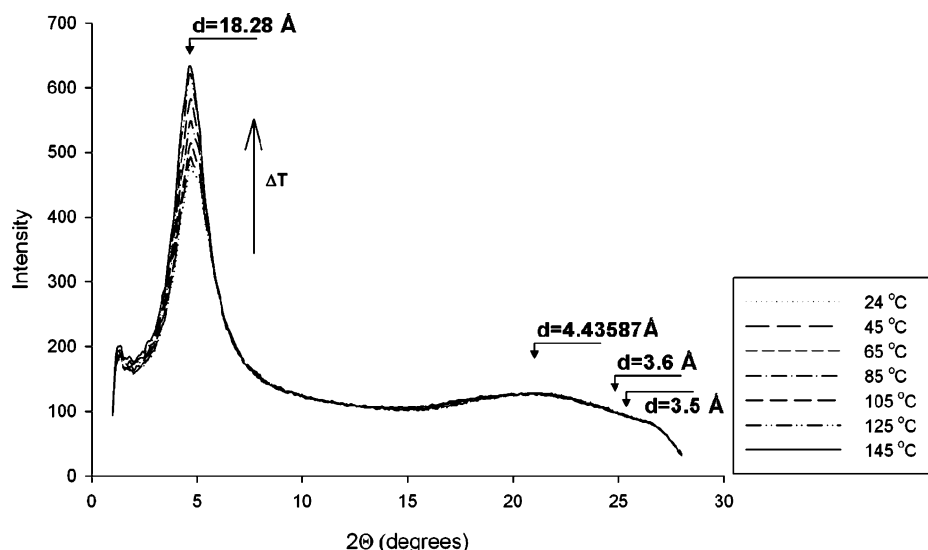


Figure 9. Variable-temperature X-ray diffraction of C_6 -HBC between 24 and 150 °C.

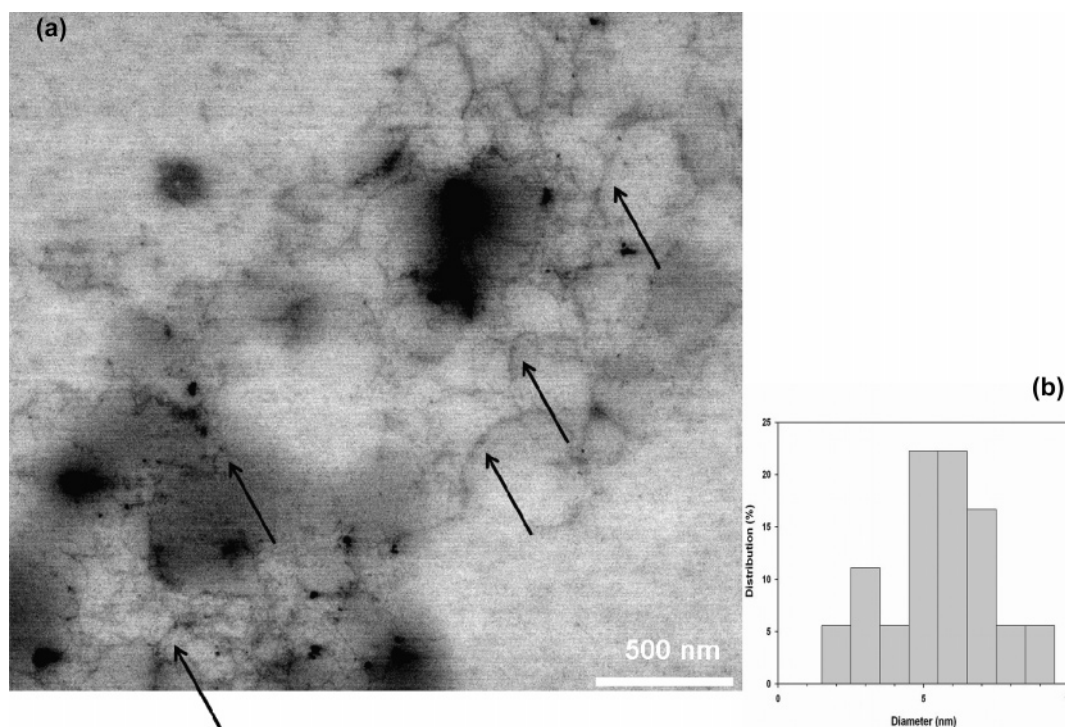


Figure 10. Scanning transmission electron microscopy of aggregates obtained from C_6 -HBC (2 mg/mL) drop-cast from toluene (a) and their size distribution (b).

agreement with previous X-ray diffraction analysis of asphaltenes.²⁶ The overlapping signals from different carbon structures present in asphaltenes and the lack of a quantitative relationship between the peak area and sample composition would make quantitative analysis of X-ray diffraction data for asphaltenes extremely unreliable, despite claims in the literature for quantitative interpretation of such data.

(23) Herwig, P.; Kayser, C. W.; Müllen, K.; Spiess, H. W. *Adv. Mater.* **1996**, *8*, 510–513.

(24) Cullity, B. D. *Elements of X-ray Diffraction*; Addison-Wesley: Reading, MA, 1978.

(25) Others have used XRD to characterize asphaltene structure and aggregation. The broadness of the peaks observed here, indicative of a mixture of conformations, makes it difficult to assess the columnar arrangement of the C_6 -HBC molecules.

(26) Ebert, L. B.; Scanlon, J. C.; Mills, D. R. *Liq. Fuels Technol.* **1984**, *2*, 257–286.

Scanning Transmission Electron Microscopy (STEM). STEM allowed the direct visualization of the behavior of C_6 -HBC at the nanometer scale. Figure 10a shows electron micrographs of C_6 -HBC solutions (2 mg/mL) in toluene deposited on carbon-coated copper grids and negatively stained using uranyl acetate.²⁷ Despite the absence of alignment, elongated one-dimensional nanostructures were detected on the carbon-coated surface. The outer diameter of these aggregates was estimated from the intensity profile average to be 6.2 ± 1.7 nm (Figure 10b), in close agreement with the crystal size determined by X-ray diffraction. These features do not correspond to the analysis of asphaltenes by TEM, which showed structures of a thickness

(27) (a) Fenniri, H.; Mathivanan, P.; Vidale, K. L.; Sherman, D. M.; Hallenga, K.; Wood, K. V.; Stowell, J. G. *J. Am. Chem. Soc.* **2001**, *123*, 3854–3855 (b) Moralez, J. G.; Ruez, J.; Yamazaki, T.; Motkuri, R. K.; Kovalenko, A.; Fenniri, H. *J. Am. Chem. Soc.* **2005**, *127*, 8307–8309.

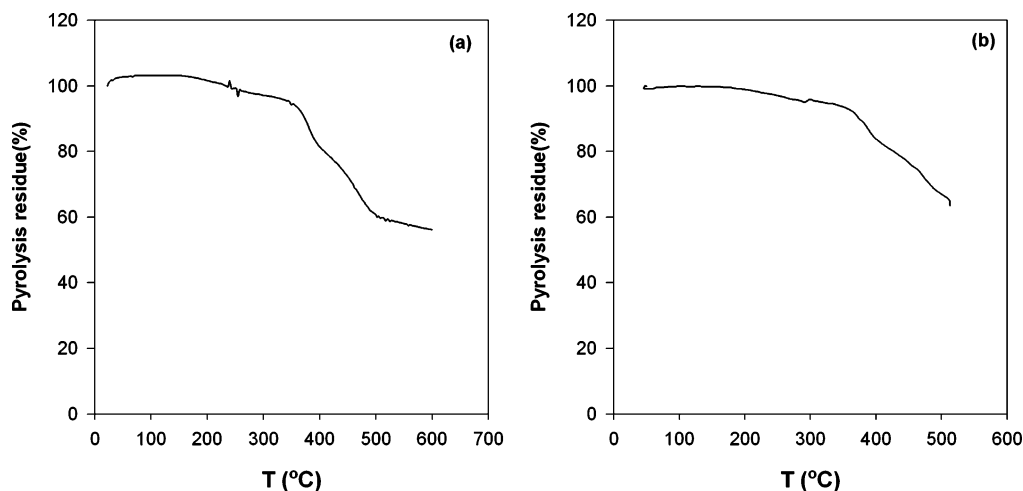


Figure 11. (a) Thermogravimetry analysis of C_6 -HBC. Heating rate = 2–5 °C/min. (b) Thermogravimetry analysis of C_6 -HBC according to ASTM-D4530-85.

of ~ 1 nm.²⁸ This discrepancy could be caused by differences in the technique used to prepare samples, but it also suggests that alkyl-HBC could be useful as a positive control in future studies of asphaltenes to show the behavior of a known alkyl aromatic compound with known association.

Coke Forming Tendency of C_6 - and C_9 -Hexabenzocoronenes. In petroleum refining, coke consists of the insoluble carbonaceous material obtained under cracking conditions. The amount of asphaltenes present in the feed has been shown to influence the yield of coke during thermal and catalytic processes. Thermogravimetry analysis of C_6 - and C_9 -HBC was carried out by heating solid samples up to 600 °C under nitrogen atmosphere at rates ranging between 2 and 5 °C/min. These heating runs indicated that both hexabenzocoronenes were stable up to 375 °C (Figure 11a). A gradual loss in weight began around 375 °C and was more pronounced at temperatures of 450–470 °C, consistent with a gradual loss of the peripheral alkyl chains followed by polymerization of the aromatic units.²⁹ Pyrolysis residues of 61 and 49% were recorded at 500 °C for C_6 - and C_9 -HBC, respectively. Microcarbon residues (MCR) for the C_6 -HBC samples according to the ASTM D4530-85 method were similar to the TGA residues at 500 °C (Figure 11b), validating the thermogravimetry analysis.

The solid line shown in Figure 12 represents the linear regression of the data plotted against the aromatic carbon content for the alkyl HBC series with the addition of data for C_{12} -HBC.²² The dashed line is the theoretical minimum MCR, assuming conversion of all aromatic carbon to graphite and the loss of all hydrogen and aliphatic carbon to the vapor. The alkyl HBC residue data consistently lie above the theoretical minimum plot, indicating that alkyl hexabenzocoronenes produce greater amounts of coke than predicted for polymerization of aromatic carbons alone. This result suggests that aliphatic carbons are incorporated into the coke obtained from alkyl HBC derivatives. Comparison of these alkyl HBC residues with the pyrolysis and

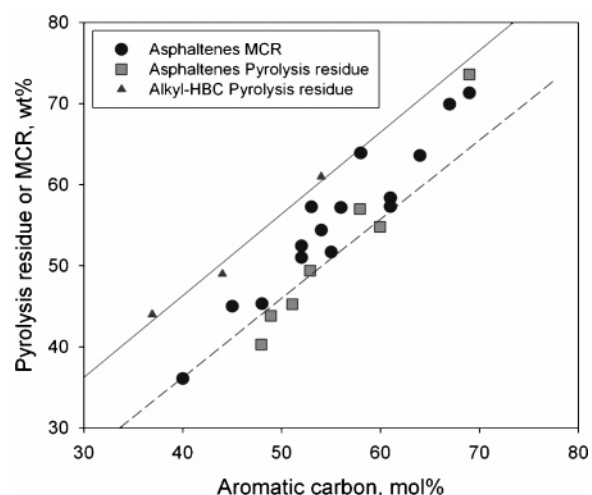


Figure 12. Comparison between the coke forming tendency of HBC model compounds and asphaltenes.³⁰

microcarbon residues for asphaltenes obtained from bitumens and heavy oils from around the world also show that alkyl HBC consistently produces more coke than authentic asphaltenes. The actual asphaltenes give less solid residue for a given aromatic carbon content than alkyl HBCs, suggesting that aromatic fragments volatilize during the coking reaction. Such loss of aromatic carbon is not possible with alkyl HBCs. These data imply either that asphaltenes contain pendant aromatic groups, as in the archipelago structure, or that a fraction of the aromatic groups are small enough to volatilize at 500 °C after sufficient side chains are cracked. The latter hypothesis is constrained by the requirement that the average boiling point of the asphaltene components must be well over 524 °C.

Conclusions

C_6 - and C_9 -hexasubstituted hexabenzocoronenes (**1a** and **1b**, respectively) were synthesized in 8 reaction steps. Microscopy, X-ray and small-angle neutron scattering, vapor pressure osmometry (VPO), NMR, and calorimetry were used to characterize the associative properties of C_6 -HBC. In particular, these studies showed that C_6 -HBC tends to form dimers in dilute solutions. The use of *o*-dichlorobenzene suppressed but did not eliminate self-association. Experimental studies at high temperatures showed that C_6 -HBC tends to self-associate at temperatures up to 400 °C, unlike simple pyrene derivatives.

(28) Sharma, A.; Groenzin, H.; Tomita, A.; Mullins, O. C. *Energy Fuels* **2002**, *16*, 490–496.

(29) Ghergel, L.; Kübel, C.; Lieser, G.; Räder, H.-J.; Müllen, K. *J. Am. Chem. Soc.* **2002**, *124*, 13130–13138.

(30) (a) Calemma, V.; Rausa, R. *J. Anal. Appl. Pyrolysis* **1997**, *40–41*, 569–584. (b) Dettman, H. D.; Salmon, S. L.; Ross, A. M.; Patmore, D. J. Physical Properties, Thermal Reactivity and Molecular Composition: Comparison of Heavy Crudes and Bitumen from Different Geographical Sources. Presented at the 52nd Canadian Chemical Engineering Conference, Vancouver, British Columbia, Canada, October 20–23, 2002; Paper 34. (c) Japanwala, S.; Chung, K. H.; Dettman, H. D.; Gray, M. R. *Energy Fuels* **2002**, *16*, 477–484.

Computational investigations supported these observations, indicating the self-association of C₆-HBC through the favorable interplay of alkyl–alkyl and π – π stacking interactions.

Acknowledgment. This research was supported by the Syncrude NSERC Industrial Research Chair in Advanced Upgrading of Bitumen. This work benefited from the use of facilities in the Intense Pulsed Neutron Source and the Chemistry Division, which is funded by the U.S. Department of Energy, Office of Basic Energy Sciences, under contract W-31-109-ENG-38 to the University of Chicago. We would like to thank Steve Pouliot from the Department of Chemical Engineering (Université Laval) for the variable-temperature X-ray measurements and Dr. Christophe Danumah for

the STEM measurements. We would particularly like to thank Pappannan Thiyagarajan and Denis Wozniak of the Intense Pulsed Neutron Source Division at Argonne National Laboratory for their assistance with the SAND instrument.

Supporting Information Available: Experimental details for VPO, ¹H NMR studies, SANS, DSC, TGA, and hot-stage microscopy, synthetic procedures, and characterization of **1a** and **1b** optimized geometries for C₆-HBC monomers. This material is available free of charge via the Internet at <http://pubs.acs.org>.

EF060130E